

NONLINEAR OPTICAL PHENOMENA

https://doi.org/10.1070/QEL17092

Normal modes of strictly resonant and quasi-resonant regimes of electromagnetically induced transparency

O.M. Parshkov

Abstract. **We report the results of a theoretical study of the evolution of a probe pulse under electromagnetically induced transparency conditions in the lambda scheme of degenerate inhomogeneously broadened quantum transitions. It is assumed that the interacting fields are elliptically polarised, and their effect on the medium can be either strictly resonant or quasi-resonant. It is shown that probe light in a medium can be represented as the sum of two normal modes, i.e. quasi-monochromatic elliptically polarised fields propagating independently of each other. The major axis of the polarisation ellipse of the normal mode of the first type is parallel, and that of the second type is perpendicular to the major axis of the polarisation ellipse of the control light. Due to the fact that velocities of normal-mode pulses are different, a single probe pulse entering a medium splits into individual pulses inside the medium, each of which transfers the energy of one of the normal modes. In the case of quasi-resonance, the splitting occurs at a shorter distance than in the case of strict resonance. If normal modes are not phase modulated at the input surface of the medium, then in the case of quasi-resonance they become phase modulated during their propagation inside the medium, whereas this does not occur in the case of strict resonance. It is shown that in the case of quasi-resonance, the phase modulation value of the mode of the second of the above types significantly exceeds that of the first type. The medium transparency for the normal mode of the first type slightly decreases with the transition from the case of strict resonance to the case of quasi-resonance, while the medium transparency for the mode of the second type decreases significantly. The total probe field, which is the sum of the normal modes, has phase modulation before it splits into mode pulses in cases of both strict resonance and quasi-resonance, even if it does not have it on the input surface.**

Keywords: *electromagnetically induced transparency, quasi-resonance, phase modulation, normal modes.*

1. Introduction

Destructive interference of population probability amplitudes of the energy levels of quantum transitions in some double resonance regimes [1] is the basis for a number of widely studied effects. Of great importance among them is stimulated Raman adiabatic transport [2] and electromagnetically induced transparency (EIT) [3 – 5]. In particular, the use of the EIT phenomenon is promising for the development of optical quantum memory systems [4], quantum communication [4, 6, 7] and quantum information systems [3 – 5] and precision magnetic measurement [8] and chronometry [9] devices. The same effect underlies the methods for producing high optical nonlinearities [5, 10] and amplifying light without population inversion [11]. The study of the specifics of EIT in various new situations is being continued. For example, the distinctive features of this phenomenon are being investigated in strongly correlated quantum gases [12], in the radiofrequency range [13], on impurities in photonic crystals [14], in the presence of nanofibre [15].

The EIT phenomenon leads to a number of effects related to polarisation characteristics of interacting fields in the presence of degeneracy of the energy levels of quantum transitions. Wielandy and Gaeta [16] and Bo Wang et al. [17] theoretically and experimentally studied the probe field polarisation plane rotation, accompanying EIT, with a change in control field intensity, and Agrawal and Dasgupta [18] and Sautenkov et al. [19] investigated the influence of a constant magnetic field on the evolution of the circular components of probe light. Linear and circular birefringence of the probe field in the case of EIT was examined theoretically and experimentally in [20]. In a theoretical study, Kis et al. [21] predicted the possibility of EIT probe field propagation in the form of two modes with different polarisation states.

In our paper [22], we reported the results of a theoretical study of birefringence accompanying EIT under elliptical polarisation of the probe and control fields at the input to a resonant medium. The investigation in this work was limited by strict resonance conditions, i.e., the coincidence of the carrier frequencies of the probe and control fields with the centre frequencies of the corresponding inhomogeneously broadened quantum transitions. The object of study in [22] was a lambda scheme of quantum transitions between $^3P_0$, $^3P_2$, $^3P_1^0$ degenerate energy levels of the ^{208}Pb isotope. In the vapours of this isotope, EIT was experimentally observed for circularly polarised laser fields [23, 24]. Analytical methods [22] demonstrate that a probe pulse in a medium can be represented as the sum of elliptically polarised normal modes propagating independently of each other.

In this paper we present the results of an analytical and numerical study of EIT on the same quantum transitions and for the same characteristics of the interacting fields as in [22], but in the case of quasi-resonance. By quasi-resonance we mean a situation where the carrier frequencies of the fields are detuned from the centre frequencies of the corresponding quantum transitions by a value comparable with the linewidths of the inhomogeneous broadening of these transitions.

O.M. Parshkov Yuri Gagarin State Technical University of Saratov, ul. Politekhnicheskaya 77, 410054 Saratov, Russia;
e-mail: oparshkov@mail.ru

Received 6 July 2019
Kvantovaya Elektronika **49** (11) 1019 – 1027 (2019)
Translated by I.A. Ulitkin

New results related to the strict resonance regime of EIT are also presented.

2. Initial equations

The lambda scheme in question is shown in Fig. 1. Levels 1, 2, 3 are identified with nondegenerate lower ($^3P_0$), threefold degenerate upper ($^3P_1^0$) and fivefold degenerate intermediate ($^3P_2$) levels of the ^{208}Pb isotope, respectively. Let ϕ_k (k = 1, 2, ..., 9) be an orthonormal basis of common eigenfunctions of energy operators, the squared angular momentum and its projection onto the z axis for an isolated atom corresponding to level 1(k = 1, M = 0), level 2 (k = 2, 3, 4, M = –1, 0, 1) and level 3 (k = 5, 6, …, 9, M = –2, –1, 0, 1, 2). Let D_1 and D_2 be the reduced electric dipole moments of 1 → 2 and 3 → 2 transitions, respectively, and ω_{210} and ω_{230} ($\omega_{210} > \omega_{230}$) be the centre frequencies of these transitions. To take into account the thermal motion of gas atoms, we introduce the quantity $T_1 = 1/\Delta_1$, where Δ_1 is the half-width (at the e^{-1} level) of the ω_{21} frequency distribution density of quantum transitions between levels 1 and 2 due to the Doppler effect.

The total electric field of two laser pulses propagating along the z axis is represented the form

$$\boldsymbol{E} = \boldsymbol{E}_1 + \boldsymbol{E}_2,$$

$$\boldsymbol{E}_l = \mu_l[\boldsymbol{e}_x\tilde{E}_{xl}\cos(\omega_l t - k_l z + \tilde{\delta}_{xl}) + \boldsymbol{e}_y\tilde{E}_{yl}\cos(\omega_l t - k_l z + \tilde{\delta}_{yl})], \quad l = 1,2, \tag{1}$$

where $\boldsymbol{E}_l$ and ω_l are the strengths and carrier frequencies of the probe (l = 1) and control (l = 2) electric fields; $\mu_l = \hbar\sqrt{2l+1}/(|D_l|T_1)$; $\boldsymbol{e}_x$ and $\boldsymbol{e}_y$ are the unit vectors of the x and y axes; $\tilde{E}_{xl}$, $\tilde{E}_{yl}$ are the amplitudes; $\tilde{\delta}_{xl}$ and $\tilde{\delta}_{yl}$ are the phase shifts of the x and y components of the probe and control fields; and $k_l = \omega_l/c$. The quantities $\tilde{E}_{xl}$, $\tilde{E}_{yl}$, $\tilde{\delta}_{xl}$, and $\tilde{\delta}_{yl}$ are real, differentiable as many times as necessary, functions of the variables s and w. The effect of the light on the medium is assumed to be quasi-resonant: $|\omega_{210} - \omega_1| \ll \omega_{210}$ and $|\omega_{230} - \omega_2| \ll \omega_{230}$.

Let f_l and g_l be the amplitudes of the left and right circular components [25] of the probe and control fields:

$$f_l = \frac{\tilde{E}_{xl}\exp(\mathrm{i}\tilde{\delta}_{xl}) - \mathrm{i}\tilde{E}_{yl}\exp(\mathrm{i}\tilde{\delta}_{yl})}{\sqrt{2}},$$

$$g_l = \frac{\tilde{E}_{xl}\exp(\mathrm{i}\tilde{\delta}_{xl}) + \mathrm{i}\tilde{E}_{yl}\exp(\mathrm{i}\tilde{\delta}_{yl})}{\sqrt{2}}.$$

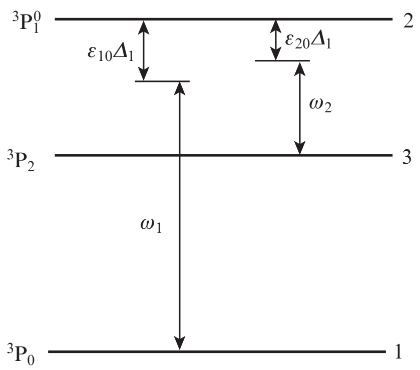

Figure 1. Lambda scheme of quantum transitions. The frequency intervals between energy levels correspond to an atom at rest and the case with $\varepsilon_{10} > 0$, $\varepsilon_{20} > 0$.

We represent the wave function Ψ of the atom in field (1) as an expansion in the basis of ϕ_k:

$$\Psi = \bar{c}_1\phi_1 + \left(\sum_{k=2}^{4}\bar{c}_k\phi_k\right)\exp(-\mathrm{i}\xi_1) + \left(\sum_{k=5}^{9}\bar{c}_k\phi_k\right)\exp[\mathrm{i}(\xi_1 - \xi_2)],$$

where $\bar{c}_k$ (k = 1, 2, ..., 9) are the probability amplitudes of quantum state population, and $\xi_l = \omega_l t - k_l z$. The normalised independent variables s and w are introduced in the form

$$s = z/z_0, \quad w = (t - z/c)/T_1,$$

where $z_0 = 3\hbar c/(2\pi N|D_1|^2 T_1\omega_{210})$; N is the concentration of atoms. Using Maxwell's and Schrödinger equations, as well as introducing the notation

$$c_1 = p_1^*\bar{c}_1, \quad c_2 = \bar{c}_2, \quad c_4 = \bar{c}_4, \quad c_5 = p_2\bar{c}_5,$$

$$c_7 = (1/\sqrt{6})p_2\bar{c}_7, \quad c_9 = p_2\bar{c}_9, \quad p_l = 2D_l/|D_l|,$$

we obtain, as a first slow envelope approximation, the system of equations:

$$\frac{\partial f_1}{\partial s} = \frac{\mathrm{i}}{\sqrt{\pi}}\int_{-\infty}^{+\infty} c_1 c_2^* \exp[-(\varepsilon_1 - \varepsilon_{10})^2]\mathrm{d}\varepsilon_1,$$

$$\frac{\partial f_2}{\partial s} = -\frac{\mathrm{i}}{\sqrt{\pi}}\xi\int_{-\infty}^{+\infty}(c_4^* c_9 + c_2^* c_7)\exp[-(\varepsilon_1 - \varepsilon_{10})^2]\mathrm{d}\varepsilon_1,$$

$$\frac{\partial g_1}{\partial s} = -\frac{\mathrm{i}}{\sqrt{\pi}}\int_{-\infty}^{+\infty} c_1 c_4^* \exp[-(\varepsilon_1 - \varepsilon_{10})^2]\mathrm{d}\varepsilon_1,$$

$$\frac{\partial g_2}{\partial s} = \frac{\mathrm{i}}{\sqrt{\pi}}\xi\int_{-\infty}^{+\infty}(c_2^* c_5 + c_4^* c_7)\exp[-(\varepsilon_1 - \varepsilon_{10})^2]\mathrm{d}\varepsilon_1,$$

$$\frac{\partial c_1}{\partial w} = -\mathrm{i}(f_1 c_2 - g_1 c_4), \tag{2}$$

$$\frac{\partial c_2}{\partial w} + \mathrm{i}\varepsilon_1 c_2 = -\frac{\mathrm{i}}{4}(f_1^* c_1 + g_2^* c_5 - f_2^* c_7) - \gamma c_2,$$

$$\frac{\partial c_4}{\partial w} + \mathrm{i}\varepsilon_1 c_4 = \frac{\mathrm{i}}{4}(g_1^* c_1 - g_2^* c_7 + f_2^* c_9) - \gamma c_4,$$

$$\frac{\partial c_5}{\partial w} + \mathrm{i}(\varepsilon_1 - \varepsilon_2)c_5 = -\mathrm{i}g_2 c_2,$$

$$\frac{\partial c_7}{\partial w} + \mathrm{i}(\varepsilon_1 - \varepsilon_2)c_7 = \frac{\mathrm{i}}{6}(f_2 c_2 - g_2 c_4),$$

$$\frac{\partial c_9}{\partial w} + \mathrm{i}(\varepsilon_1 - \varepsilon_2)c_9 = \mathrm{i}f_2 c_4,$$

where

$$\varepsilon_1 = (\omega_{21} - \omega_1)/\Delta_1; \quad \varepsilon_2 = \varepsilon_{20} + \beta(\varepsilon_1 - \varepsilon_{10});$$

$$\xi = 0.6\beta|D_2/D_1|^2; \quad \beta = \omega_{230}/\omega_{210};$$

$\gamma = T_1/(2\tau)$; τ is the radiative lifetime of the $^3P_1^0$ level. The parameters ε_{10} and ε_{20} describe the degree of the nonresonance effect of the light on the medium and are determined by the formulas

$$\varepsilon_{10} = (\omega_{210} - \omega_1)/\Delta_1,\ \ \varepsilon_{20} = (\omega_{230} - \omega_2)/\Delta_1 \qquad (3)$$

(Fig. 1). These quantities are hereinafter referred to as resonance detunings. The resonance is strict if $\varepsilon_{10} = \varepsilon_{20} = 0$. System (2) is formally identical to the system of equations used in [22]. However, the relationship between the parameters ε_{10} and ε_{20} is more complicated than in [22], where it was assumed that strict resonance conditions were satisfied.

Let a_l, α_l and γ_l be the parameters of the polarisation ellipse (PE) of the probe ($l = 1$) and control ($l = 2$) light. Here, a_l is the semimajor axis of the PE, measured in units of μ_l; α_l is the angle of its inclination to the x axis ($0 \leqslant \alpha_l \leqslant \pi$); and γ_l is the compression parameter ($-1 \leqslant \gamma_l \leqslant +1$) [26]. The value of $|\gamma_l|$ determines the ratio of the minor axis of the PE to its major axis. Negative and positive values of γ_l correspond to the right and left elliptical polarisations, respectively [25].

The $\tilde{E}_{ul}$ and $\tilde{\delta}_{ul}$ ($u = x, y$) values in formulas (1) can be represented as

$$\tilde{E}_{ul} = E_{ul}\exp(\mathrm{i}\varphi_{ul}),\ \ \tilde{\delta}_{ul} = \delta_{ul} + \varphi_{ul},$$

where $E_{ul} = |\tilde{E}_{ul}|$; $\varphi_{ul} = 0$, if $\tilde{E}_{ul} \geqslant 0$; and $\varphi_{ul} = -\pi$, if $\tilde{E}_{ul} < 0$. The function $\delta_{xl}(\delta_{yl})$ experiences jumps by $\pm\pi$ at the nodal points, i.e., at points (s, w), where $\tilde{E}_{xl}(\tilde{E}_{yl})$ reverses its sign. Between these points, the function $\delta_{xl}(\delta_{yl})$ is continuous. The values of E_{ul} and δ_{ul} are uniquely related to the PE parameters of the corresponding light and to one of the phase shifts [22]. Therefore, specifying the parameters a_l, α_l, γ_l, and also one of the quantities δ_{xl} and δ_{yl} is equivalent to the definition of the field by formula (1).

The initial conditions were imposed on the values of the populations of quantum states at the initial instant of time ($w = 0$) and had the form

$$c_1 = 2,\ c_4 = c_5 = c_7 = c_9 = 0,\ w = 0,\ s \geqslant 0,\ \varepsilon_1 \in (-\infty, +\infty). \qquad (4)$$

These conditions correspond to the case when, before the interaction of the light with the medium, all atoms are at the lower energy level of the lambda scheme. The boundary conditions for system (2) were set as follows:

$$a_l = a_{l0},\ \alpha_l = \alpha_{l0},\ \gamma_l = \gamma_{l0},\ \delta_{xl} = \delta_{xl0},\ s = 0,\ w \geqslant 0, \qquad (5)$$

where a_{l0}, α_{l0}, γ_{l0}, and δ_{xl0} are functions of w that describe the evolution of a_l, α_l, γ_l, and δ_{xl} on the input surface ($s = 0$) of the resonant medium. It was also assumed that $a_{10}(0) = 0$. Taking into account the fact that an initial population of levels that form a quantum transition quasi-resonant to the control field is absent, this means that the interaction of the light with the medium begins at time moment $w = 0$.

3. Normal modes and phase modulation

Let the probe field be much weaker than the control field, so that the condition

$$\sqrt{E_{x1}^2 + E_{y1}^2}\Big/\sqrt{E_{x2}^2 + E_{y2}^2} \ll 1$$

is met. Let also the control light be elliptically polarised. In [22], we showed for the case of strict resonance that the probe field in the medium, described by the solution of the boundary value problem (2), (4), (5) and hereinafter referred to as the total probe field, is the sum of two fields with constant polarisation characteristics α_l and γ_l. These light fields are elliptically polarised, and the major axis of the PE of one of them is parallel, and the other is perpendicular to the major axis of the PE of the control field. The PE compression parameters of the modes are identical in modulus and opposite in sign. The probe light of the first type is called in [22] the parallel normal mode, and that of the second type is called the perpendicular normal mode. The modes do not interact with each other when propagating in a medium. The boundary conditions for each mode have the form of (5) for $l = 1$, and the values of $a_{10}, \alpha_{10}, \gamma_{10}$, and δ_{x10} are determined by their values for the total probe field at the input surface ($s = 0$). The procedure for finding the boundary conditions for each normal mode in the absence of phase modulation of the total probe field at the input surface of the medium is described in [22].

The justification of the above statements presented in [22], in fact, does not depend on the type of coupling between the resonance detunings ε_{10} and ε_{20}. Therefore, these statements remain true for quasi-resonant conditions. However, the evolution of normal modes, as well as the total field in a medium in the case of quasi-resonance, differs markedly from their evolution in the case of strict resonance. In particular, we will show below that in the case of strict resonance, normal modes are not phase modulated although the total probe field has phase modulation at some stages. In the case of quasi-resonance, phase modulation is present both in the modes and in the total probe field.

In representing the fields in the form of (1), the presence of phase modulation for the x component of the parallel mode in the medium means that the function $\tilde{\delta}_{x1}^{(1)}$ is not constant. Let us consider in more detail the conditions for the absence of phase modulation for the parallel normal mode. Its evolution can be described by the system of equations [22]:

$$\frac{\partial g_1^{(1)}}{\partial s} = \frac{2\mathrm{i}}{\sqrt{\pi}}\,\frac{1}{\kappa^2+1}\int_{-\infty}^{+\infty} U_1^* \exp[-(\varepsilon_1 - \varepsilon_{10})^2]\,\mathrm{d}\varepsilon_1,$$

$$\frac{\partial U_1}{\partial w} + \mathrm{i}\varepsilon_1 U_1 = -\frac{\mathrm{i}}{2}(1+\kappa^2)g_1^{(1)*} - \frac{\mathrm{i}}{4}g_2^* V_1 - \gamma U_1, \qquad (6)$$

$$\frac{\partial V_1}{\partial w} + \mathrm{i}(\varepsilon_1 - \varepsilon_2)\,V_1 = -\mathrm{i}g_2 q_1 U_1\,,$$

where κ and q_1 are constant values;

$$U_1 = \kappa c_2 - c_4;\ \ V_1 = \kappa c_5 - (\kappa_2\kappa + 1)c_7 + \kappa_2 c_9;$$

and κ_2 is a constant value. (Hereafter, superscripts 1 and 2 correspond to the characteristics of the parallel and perpendicular normal modes, respectively.) The value of $g_1^{(1)}$ can be represented as

$$g_1^{(1)} = \tilde{g}_{x1}^{(1)}\exp(\mathrm{i}\tilde{\delta}_{x1}^{(1)}), \qquad (7)$$

where $\tilde{g}_{x1}^{(1)}$ и $\tilde{\delta}_{x1}^{(1)}$ are real, differentiable enough times, functions of s and w.

The boundary conditions for system (6) are determined by boundary conditions (4) and (5) for the total probe field:

$$g_1^{(1)}(0,w) = \tilde{g}_{x10}^{(1)}\exp\left(\mathrm{i}\tilde{\delta}_{x10}^{(1)}\right), U_1(0,w) = V_1(0,w) = 0\,,\ w \geqslant 0, \quad (8)$$

$$g_1^{(1)}(s,0) = U_1(s,0) = V_1(s,0) = 0,\ s \geqslant 0. \quad (9)$$

Here $\tilde{g}_{x10}^{(1)}$ and $\tilde{\delta}_{x10}^{(1)}$ are the specified real functions of the argument w.

Suppose that $\tilde{\delta}_{x1}^{(1)} = \bar{\delta}$, where $\bar{\delta}$ is a constant. This means that the parallel normal mode is not phase modulated. We introduce the notations

$$\varepsilon = \varepsilon_1 - \varepsilon_{10},\ \Delta_0 = \varepsilon_{10} - \varepsilon_{20},$$

where Δ_0 is the detuning from the resonance of the Raman scattering type, and we also set

$$P = \mathrm{i}U_1^*\exp(-\mathrm{i}\tilde{\delta}_{x1}^{(1)}),\quad Q = \mathrm{i}V_1^*\exp(-\mathrm{i}\tilde{\delta}_{x1}^{(1)}).$$

Then, using expression (7), the boundary value problem (6), (8), (9) can be represented as

$$\frac{\partial\tilde{g}_{x1}^{(1)}}{\partial s} = \frac{2}{\sqrt{\pi}}\frac{1}{\kappa^2+1}\int_{-\infty}^{+\infty}P\exp(-\varepsilon^2)\,\mathrm{d}\varepsilon, \quad (10)$$

$$\frac{\partial P}{\partial w} - \mathrm{i}(\varepsilon+\varepsilon_{10})P = -\frac{1}{2}(1+\kappa^2)\tilde{g}_{x1}^{(1)} + \frac{\mathrm{i}}{4}g_2Q - \gamma P, \quad (11)$$

$$\frac{\partial Q}{\partial w} - \mathrm{i}(\beta\varepsilon+\Delta_0)Q = \mathrm{i}g_2^*q_1P, \quad (12)$$

$$\tilde{g}_{x1}^{(1)}(0,w) = \tilde{g}_{x10}^{(1)}(w),\quad P(0,w) = Q(0,w) = 0\,,\ w \geqslant 0, \quad (13)$$

$$\tilde{g}_{x1}^{(1)}(s,0) = P(s,0) = Q(s,0) = 0\,,\ s \geqslant 0. \quad (14)$$

The functions P and Q depend parametrically on ε. However, boundary conditions (13) and (14) are the same for P and Q, corresponding to different values of ε.

According to (11), the value of P is generally not real, so that the integral on the right-hand side of equation (10) may turn out to be an imaginary value. Moreover, the left-hand side of this equation is real. This means that in the general case a solution of form (7) with a constant value of the phase shift $\tilde{\delta}_{x1}^{(1)}$ does not exist and the x component of the parallel normal mode will be phase modulated.

One possible exception is the case of strict resonance conditions for the probe and control fields:

$$\varepsilon_{10} = \Delta_0 = 0. \quad (15)$$

To prove this fact, we write equation (10) in the form

$$\frac{\partial\tilde{g}_{x1}^{(1)}}{\partial s} = \frac{2}{\sqrt{\pi}}\frac{1}{\kappa^2+1}\int_0^{+\infty}[P(\varepsilon)+P(-\varepsilon)]\exp(-\varepsilon^2)\,\mathrm{d}\varepsilon. \quad (16)$$

Here $P(\varepsilon)$ and $P(-\varepsilon)$ are the functions satisfying equations (11) and (12) and boundary conditions (13) and (14) for the detuning parameters ε and $-\varepsilon$. It is easy to show that boundary value problems for a pair of functions $P(-\varepsilon)$ and $Q(-\varepsilon)$ completely coincide with the boundary value problem for a pair of functions $P^*(\varepsilon)$ and $Q^*(\varepsilon)$. However, this means that $P(-\varepsilon) = P^*(\varepsilon)$; therefore,

$$P(\varepsilon) + P(-\varepsilon) = P(\varepsilon) + P^*(\varepsilon) = 2\mathrm{Re}P(\varepsilon).$$

Thus, the right-hand side of equation (16) is a real value. The solution of the boundary value problem (10)–(14) and the use of formula (7) at $\tilde{\delta}_{x1}^{(1)} = \bar{\delta}$ then determines the x component of the parallel mode without phase modulation.

We can show that the function $g_1^{(1)}$ in equation (6) has the form

$$g_1^{(1)} = \tilde{g}_{y1}^{(1)}\exp\{\mathrm{i}[\tilde{\delta}_{y1}^{(1)} - \delta_1^{(1)}]\},$$

where $\tilde{g}_{y1}^{(1)}$ and $\tilde{\delta}_{y1}^{(1)}$ are real continuous functions of s and w; and $\delta_1^{(1)}$ is a constant. With the arguments similar to those given above, we conclude that, under conditions (15), the y component of the parallel mode is also devoid of phase modulation. The absence of phase modulation for the components of the perpendicular normal mode is justified similarly.

Let us enumerate the conditions necessary for the absence of phase modulation for normal modes in the medium. Firstly, this is the absence of phase modulation for the total probe light at the input surface of the medium. Moreover, according to [22], the light of normal modes at the entrance to the medium will also not be phase modulated. Secondly, this is the zero population of the upper levels of the lambda scheme until the moment of its interaction with the fields of the probe and control light. Thirdly, this is the fulfilment of strict resonance conditions (15).

In the general case, the light of normal modes is phase modulated. Using the results presented in [22], we can obtain expressions relating the phase shifts of the components of the mode of each type at all spatiotemporal points:

$$\tilde{\delta}_{y1}^{(1)} = \tilde{\delta}_{x1}^{(1)} + \frac{\pi}{2} + 2\pi m,\ \tilde{\delta}_{y1}^{(2)} = \tilde{\delta}_{x1}^{(1)} - \frac{\pi}{2} + 2\pi m',\ \ m, m' \in \mathbb{Z}, \quad (17)$$

with the phase shifts being continuous functions of the variables s and w.

4. Numerical results

We specify boundary conditions (5) as follows:

$$\begin{aligned} &a_{10} = 0.2\,\mathrm{sech}[(w-300)/50], \\ &\alpha_{10} = \pi/6,\ \gamma_{10} = -0.5,\ \delta_{x10} = 0, \end{aligned} \quad (18)$$

$$a_{20} = 6.516,\ \alpha_{20} = 0,\ \gamma_{20} = -0.3,\ \delta_{x20} = 0. \quad (19)$$

Conditions (18) describe the input pulse of the total probe light with a duration of 15 ns and a peak intensity of 65 W cm^{-2}. The intensity of the control light according to (19) is constant and is approximately 20 kW cm^{-2}. The peak intensity of the input probe pulse is more than 300 times less than the intensity of the control field; therefore, the situation described by formulas (18) and (19) refers to the case of weak probe light. (The rationale for choosing the values of the parameters of the resonant medium and input light is given in detail in [27].)

Using the technique described in [22], we obtain the boundary conditions for normal modes on the input surface of the medium:

$$a_{10}^{(1)} = 0.0720\,\mathrm{sech}[(w-300)/50],$$
$$\alpha_{10}^{(1)} = 0,\ \gamma_{10}^{(1)} = 0.7417,\ \delta_{x10}^{(1)} = -0.4993 \tag{20}$$

for the parallel normal mode and

$$a_{10}^{(2)} = 0.1645\,\mathrm{sech}[(w-300)/50],$$
$$\alpha_{10}^{(2)} = \pi/2,\ \gamma_{10}^{(2)} = -0.7417,\ \delta_{x10}^{(2)} = 0.2884 \tag{21}$$

for the perpendicular mode. For the modes of both types, the parameters of the input control light are given by formulas (19). In addition to conditions (19)–(21), the evolution of the total probe and normal-mode fields in a medium depends on the values of ε_{10} and ε_{20} determined by formulas (3).

4.1. Strict resonance

We assume that strict resonance conditions are satisfied: $\varepsilon_{10} = \varepsilon_{20} = 0$. The time evolution of a_1, α_1 and γ_1 of the total probe field for several fixed distances s is shown in Fig. 2. According to Figs 2b–2d, the splitting of the input pulse of the total probe field into two separate pulses becomes noticeable at distances $s > 1500$. Since the polarisation characteristics α_1 and γ_1 in the region where the pulse is located at the initial stage of its splitting (Fig. 2b) change significantly, the probe light is not elliptically polarised. (The jumps in the value of α_1 from π to 0 occur due to the limitation of the range of α_1 values.) At a large distance (Fig. 2d) the polarisation characteristics in the region where both pulses are located are constant, with $\alpha_1 = \pi$ and $\gamma_1 = 0.7417$ for the left pulse and $\alpha_1 = \pi/2$ and $\gamma_1 = -0.7421$ for the right pulse. These values are in good agreement with those in formulas (20) and (21) (taking into account that $\alpha_1 = 0$ and $\alpha_1 = \pi$ describe the same position of the major axis of the polarisation ellipse). Therefore, the left pulse in Fig. 2d shows a parallel normal mode of the light field, and the right one shows a perpendicular normal mode.

Figure 3 illustrates the evolution of a_1 together with the evolution of phase shifts $\tilde{\delta}_{x1}$ and $\tilde{\delta}_{y1}$ for two distances s. One can see from Fig. 3a that, before the pulse splits into normal modes, the phase shifts are not constant in the region where the probe field energy is concentrated, and, therefore, the probe light is phase modulated. To explain this fact, let $s_0 \geqslant 0$ be a fixed distance s. The total field at s_0 is the sum of the normal mode fields at the same point. The mode fields are amplitude modulated (see Section 3) rather than phase modulated, since the major axes of the PE of the modes at s_0 depend on w. Elementary considerations show that the sum of the mode fields at point s_0 will not be phase modulated only if the condition $a_1^{(1)}(s_0, w) = \eta a_1^{(2)}(s_0, w)$ is met, where η is a constant. According to (20) and (21), this condition is satisfied at $s_0 = 0$, which means that phase modulation of the total probe field is absent at the input surface in accordance with the constancy of the value of δ_{x10} in (18). However, due to the difference in the velocities of the pulses of the normal modes and their varying degrees of deformation during propagation to a distance $s_0 > 0$, this condition is violated. This means that the sum of the normal modes, i.e., the total probe field, is phase modulated at $s_0 > 0$.

At a large distance, after the input probe pulse splits into normal-mode pulses (Fig. 3b), phase shifts are constant in the region where the pulse of each mode is located. Moreover, in

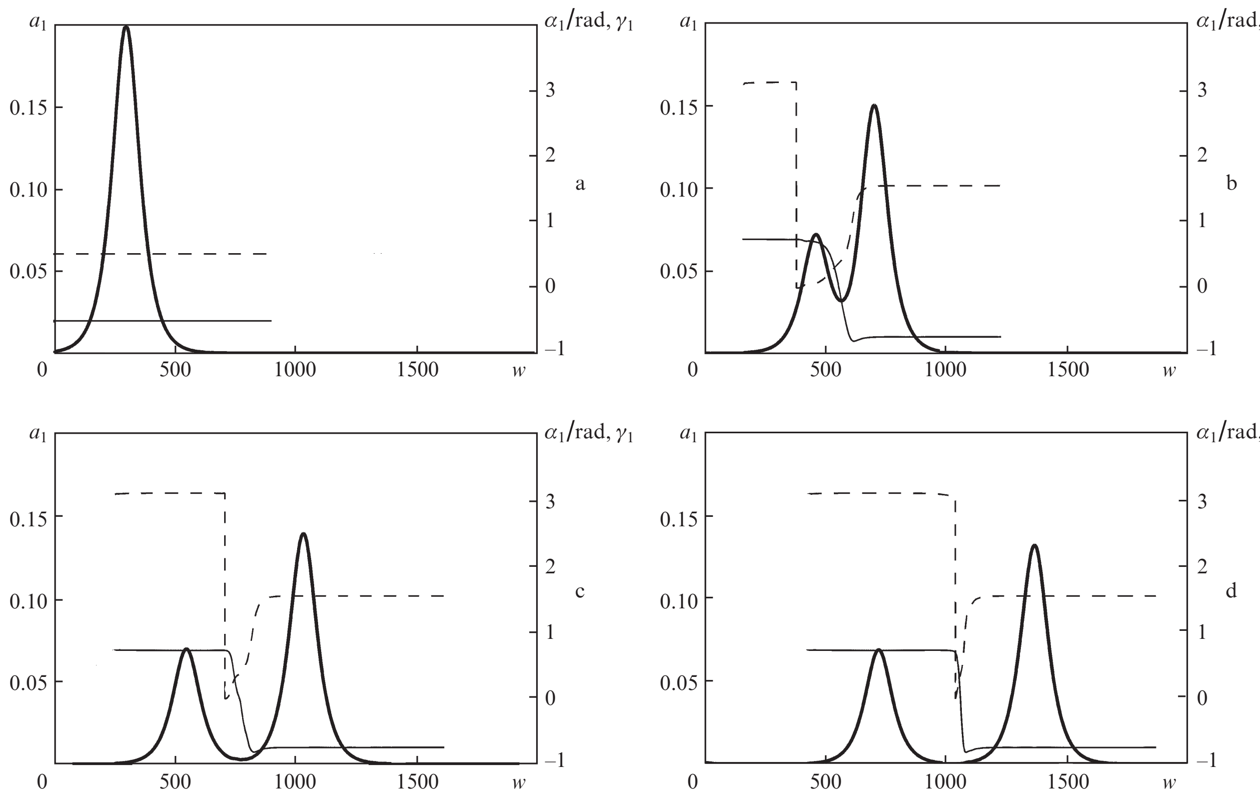

Figure 2. Evolution of the total probe field characteristics a_1 (thick solid curves), α_1 (dashed curves) and γ_1 (thin solid curves) in a medium at s = (a) 0, (b) 1500, (c) 3000 and (d) 4000.

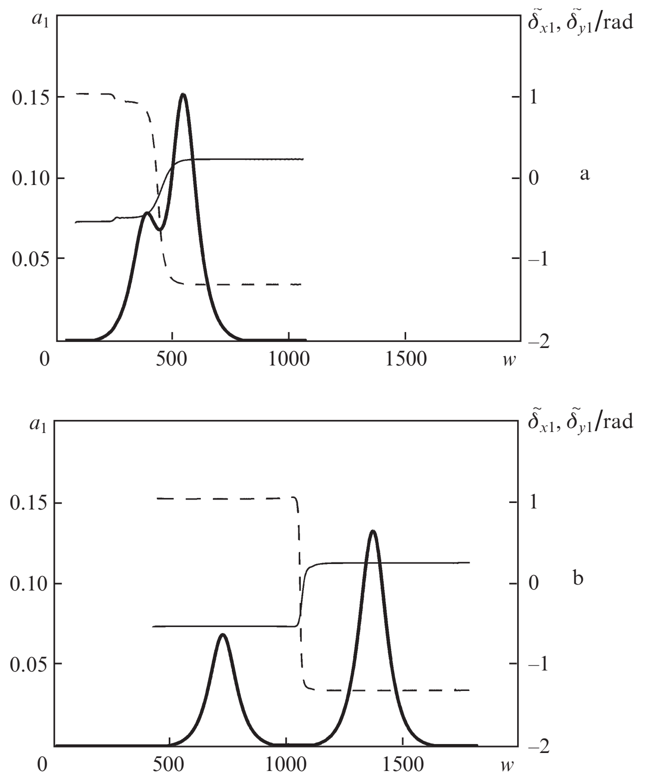

Figure 3. Evolution of a_1 (thick solid curves), $\tilde{\delta}_{x1}$ (thin solid curves) and $\tilde{\delta}_{y1}$ (dashed curves) of the total probe field at s = (a) 1000 and (b) 4000.

the region of the left pulse (parallel mode) $\tilde{\delta}_{x1} = -0.5014$, while in the region of the right pulse (perpendicular mode) $\tilde{\delta}_{x1} = 0.2793$. These values are close to the values of $\delta_{x10}^{(1)}$ and $\delta_{x10}^{(2)}$ specified in (19) and, (20). In addition, the calculation confirms that the phase shifts of both modes satisfy relations (17) at $m = m' = 0$.

4.2. Quasi-resonance

We assume that $\varepsilon_{10} = -0.3$ and $\varepsilon_{20} = 0.6$, keeping the boundary conditions (18) and (19) unchanged. This situation corresponds to the quasi-resonant interaction of the fields with the medium and will be described below in more detail. The evolution of a_1, α_1 and γ_1 for the total probe field at several fixed distances s is shown in Fig. 4. Near the input surface (Fig. 4 b), as in the case of strict resonance, the total probe light is not elliptically polarised. However, in the case of quasi-resonance, the total probe pulse splits into normal-mode pulses at much shorter distances (s = 500, Fig. 4b) than in the case of strict resonance (s = 1500, see Fig. 2b). During the splitting, three pulses arise: pulse *1* and poorly separated pulses *2* and *3* (Figs 4b–4d). The values of α_1 and γ_1 in the region of pulse *1* and pulses *2* and *3* are close to the values typical of normal modes specified in formulas (20) and (21). It follows that pulse *1* in Figs 4b–4d is a parallel normal-mode field, and pulses *2* and *3* are perpendicular normal-mode fields. Recall that in the case of strict resonance, each normal mode was represented as a single bell-shaped pulse (see Fig. 2).

Figure 5 shows the evolution of a_1 together with the evolution of phase shifts $\tilde{\delta}_{x1}$ and $\tilde{\delta}_{y1}$ for two distances s. The jumps in $\tilde{\delta}_{x1}$ and $\tilde{\delta}_{y1}$ are equal to $\pm 2\pi$ and are due to the limitation of the range of values of these quantities by 2π.

The change in phase shifts over time, shown in Fig. 5, means the presence of phase modulation of the total probe

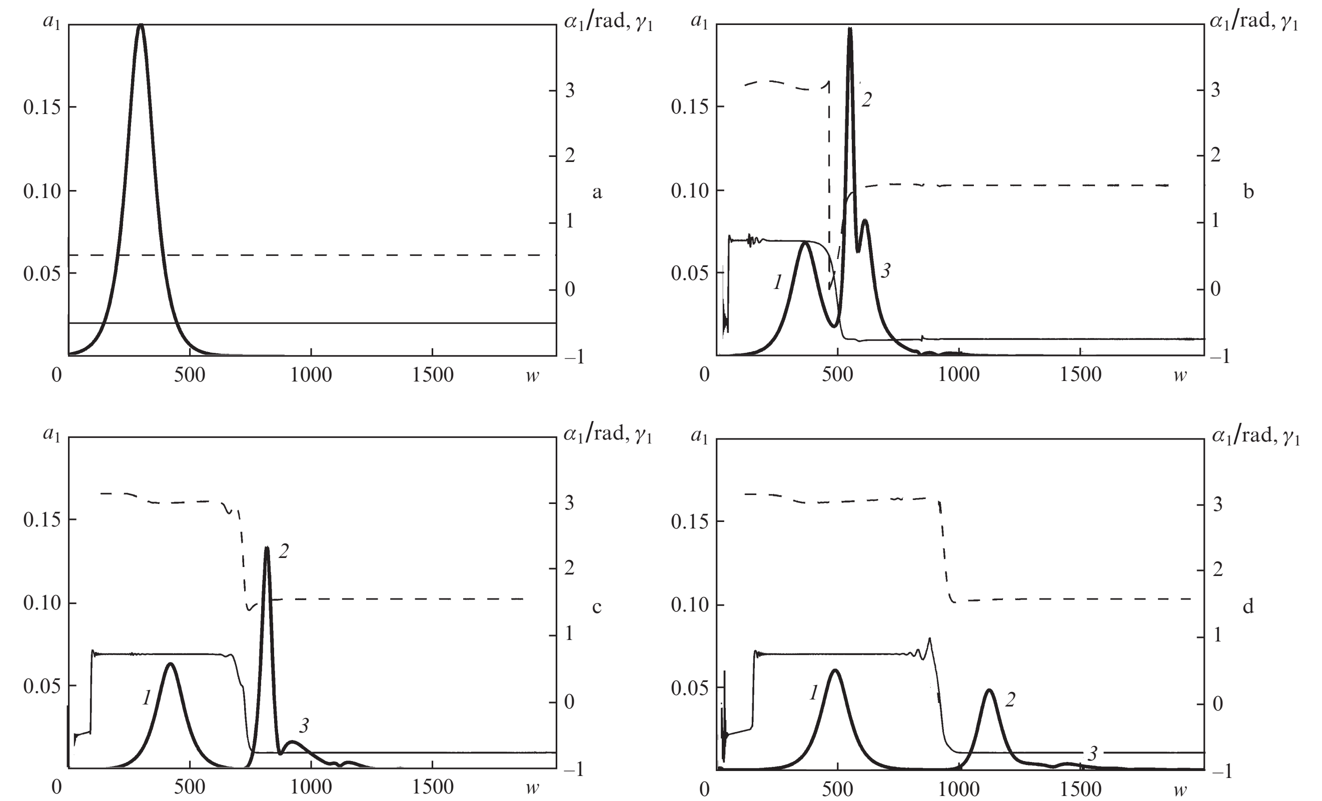

Figure 4. Evolution of the total probe field characteristics a_1 (thick solid curves), α_1 (dashed curves) and γ_1 (thin solid curves) in a medium at s = (a) 0, (b) 500, (c) 1000 and (d) 1500. Curve *1* is a parallel mode, and curves *2* and *3* are a perpendicular mode.

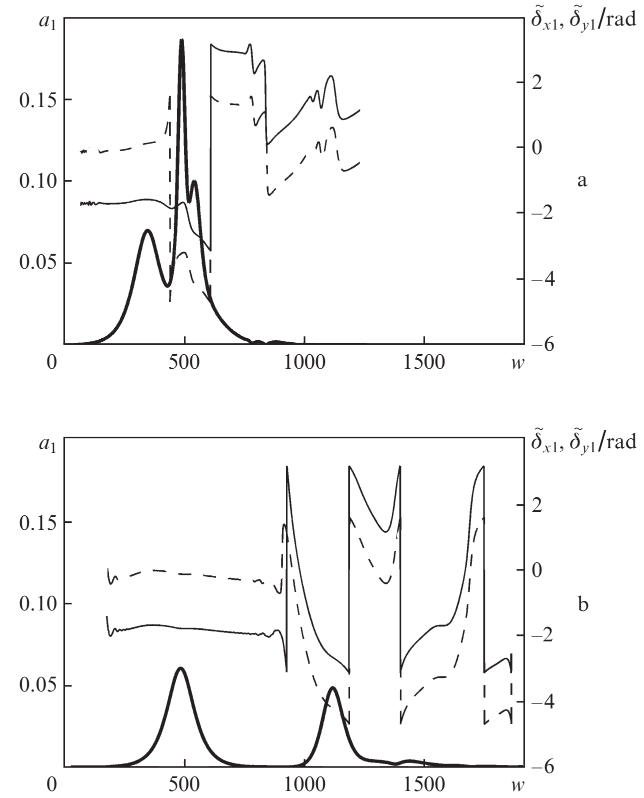

Figure 5. Evolution of a_1 (thick solid curves), $\tilde{\delta}_{x1}$ (thin solid curves) and $\tilde{\delta}_{y1}$(dashed curves) of the total probe field at s = (a) 400 and (b) 1500.

light at both small and large distances inside the medium. Moreover, at distances s sufficient for the complete splitting of the input probe pulse (Fig. 5b), $\tilde{\delta}_{x1}$ and $\tilde{\delta}_{y1}$ in the region of normal modes are related by expressions (17) at $m = m' = 0$. This fact agrees with the conclusions of the analytical theories of normal modes. However, at small distances (Fig. 5a), expressions (17) are not satisfied in the region of the total probe field.

The boundary conditions for normal modes that form the total probe light in the medium have the form of (20), (21). The calculation showed that, in accordance with the conclusions of the analytic theory, the polarisation characteristics $\alpha_1^{(i)}$ and $\gamma_1^{(i)}$ $(i = 1, 2)$ of the normal modes do not change during their propagation, remaining equal to their values at the input to the medium. Therefore, the curves describing the results of calculating these characteristics are not presented. Figure 6 shows curves demonstrating the evolution of the amplitude $(a_1^{(i)})$] and phase $[(\tilde{\delta}_{x1}^{(i)})]$ characteristics of normal modes. Figure 6a demonstrates the modes on the input surface of the medium, where, according to (20), (21), they are not phase modulated (see curves *2* in Fig. 6a). Inside the medium, as follows from Figs 6b–6d, phase shifts $\tilde{\delta}_{x1}^{(i)}$ are variables in each mode emission region. However, a change in the phase shift $\tilde{\delta}_{x1}^{(1)}$ of the parallel mode is extremely small (dashed curves *2* in Figs 6b–6d), so that the parallel mode can almost be considered devoid of phase modulation at each fixed distance s.

The phase modulation of the perpendicular normal mode is much stronger than that of the parallel mode (cf. solid and dashed curves *2* in Figs 6b–6d). The energy of the perpen-

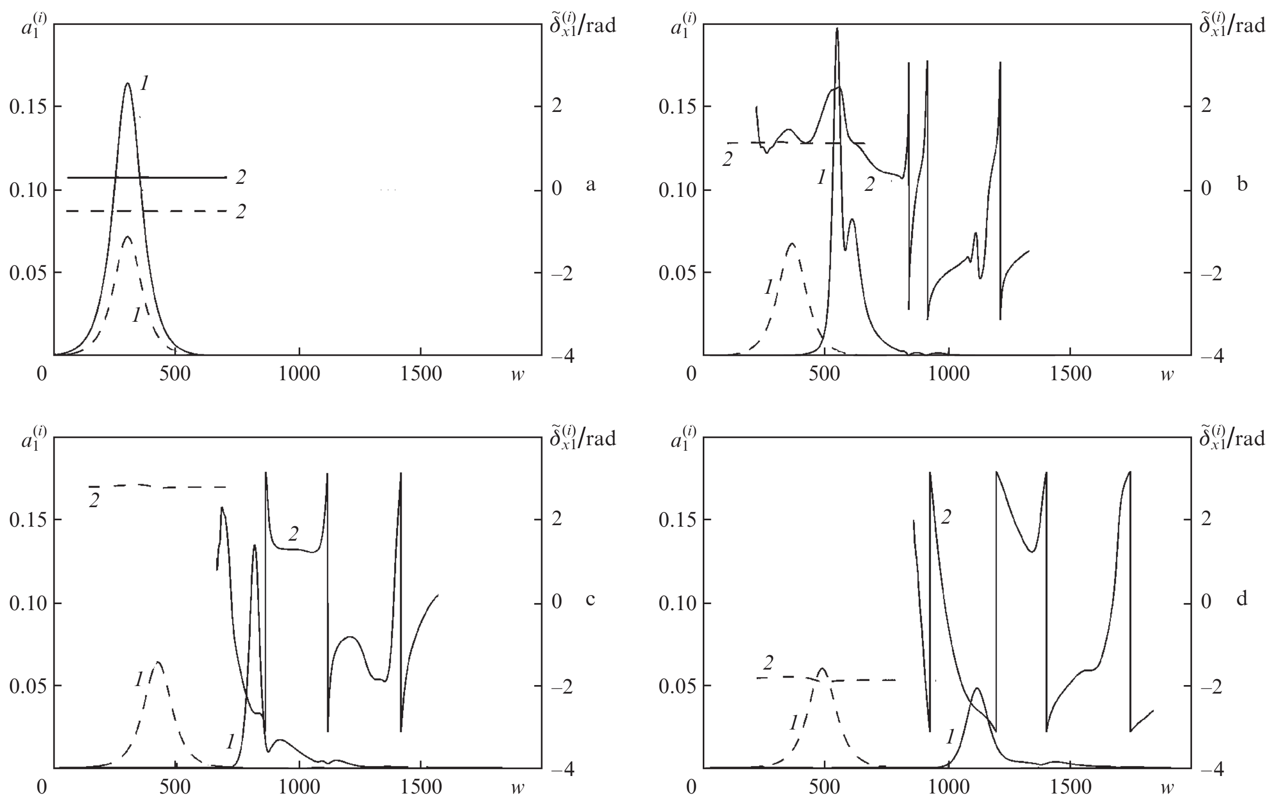

Figure 6. Evolution of (*1*) amplitudes $a_1^{(i)}$ and (*2*) phase shifts $\tilde{\delta}_{x1}^{(i)}$ of normal parallel (dashed curves) and perpendicular (solid curves) modes in a medium at s = (a) 0, (b) 500, (c) 1000 and (d) 1500.

dicular mode is contained in two poorly separated pulses, which were mentioned above. We will call the larger of them the main part of the mode, and the smaller – the secondary. Let us consider the main part of the mode at a distance $s = 1500$. According to Fig. 6d, in the region of the main part of the mode, the value of $\partial\tilde{\delta}_{x1}^{(2)}/\partial w$ is negative and, therefore, the x component of the main part of the mode has a negative chirp. The second of conditions (17) yields $\partial\tilde{\delta}_{y1}^{(2)}/\partial w = \partial\tilde{\delta}_{x1}^{(2)}/\partial w$. Therefore, the instantaneous frequencies of the x and y components of the main part of the perpendicular mode are the same at each spatiotemporal point (s, w), so that both components have the same negative chirp.

To estimate the magnitude of the chirp, we note that the instantaneous intensity $I_1^{(2)}$ of the perpendicular normal mode at fixed s and w is proportional to the square of $a_1^{(2)}(s, w)$ [22]. The calculations showed that at $s = 1500$ the dependence of the intensity $I_1^{(2)}$ of the main pulse on w is a bell-shaped curve and describes a perturbation with a duration of 85 (in units of w) at the e^{-1} level of the maximum intensity $I_{1m}^{(2)}$. Let us approximate the dependence of $I_1^{(2)}$ on w for $s = 1500$ by a Gaussian function that describes a pulse with such a duration. Then it can be shown that over a period of time during which the condition $I_1^{(2)} \geqslant 0.1 I_{1m}^{(2)}$ is satisfied, the change in the instantaneous frequency $\tilde{\omega}_1^{(2)}$ defined by the formula

$$\tilde{\omega}_1^{(2)} = \omega_1 + \frac{1}{T_1}\frac{\partial\tilde{\delta}_{x1}^{(2)}}{\partial w},$$

is approximately 15% in absolute value of the width of the spectral contour of the main part of the perpendicular mode at the e^{-1} level. This value of the instantaneous frequency deviation means that the phase modulation of the main part of the normal mode makes a significant contribution to the formation of the contour of its spectral intensity.

The maximum intensity of the secondary part of the pulse of the perpendicular mode is approximately 170 times less than the maximum intensity of its main part. Therefore, allowance for this part practically does not affect the shape of the Fourier spectrum of the light of the entire perpendicular mode. It is worth noting that in the region of the secondary part, the chirp is positive, and the magnitude of the instantaneous frequency deviation in absolute vale is approximately the same as that of the main part of the perpendicular mode.

We denote by $F(s)$ the total energy transferred by the probe field through the unit area of the wavefront at a distance s from the input surface. We call the quantity $T(s) = F(s)/F(0)$ the transmission of probe light at a distance s. Figure 7 shows the transmission curves for normal modes in cases of strict resonance and quasi-resonance. Comparing curves *1* and *2*, as well as curves *3* and *4*, we conclude that in both cases the parallel normal mode experiences less energy losses than the perpendicular one during propagation. On the other hand, it follows from Fig. 7 that in the case of quasi-resonance, the energy losses of the modes during propagation exceed such losses in the case of strict resonance. The decrease in transmission is especially pronounced in the evolution of the perpendicular normal mode. In particular, its light in the case of quasi-resonance (curve *4* in Fig. 7) is almost completely absorbed by the medium at a distance $s \approx 2000$.

Note that in the absence of a control field, weak light, whose frequency is equal to the frequency of the probe field, is almost completely absorbed when the distance s is of the order of several units. Therefore, we can assume that in the above cases the efficiency of the EIT phenomenon is quite large.

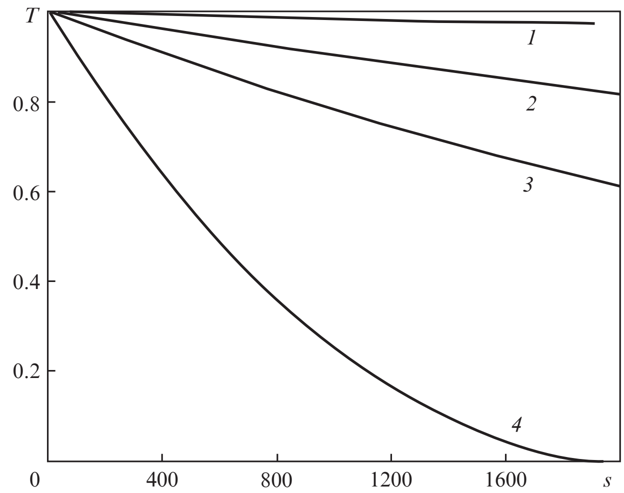

Figure 7. Transmission curves for (*1*, *3*) parallel and (*2*, *4*) perpendicular modes in the cases of (*1*, *2*) strict resonance and (*3*, *4*) quasi-resonance.

5. Conclusions

We have shown that in the case of quasi-resonance under the condition that the probe field is sufficiently weak compared to the control field, the total probe light in the medium can be represented as the sum of normal modes propagating independently of each other. The polarisation parameters of normal modes do not change during their propagation, so that the modes are elliptically polarised. The major axis of the PE of the first of the normal modes (parallel mode) is parallel, and of the second (perpendicular mode) is perpendicular to the major axis of the PE of the control field, while the compression parameters of the PE of the modes are opposite in sign. In the case of strict resonance and in the absence of phase modulation of normal modes on the input surface of the medium, the normal modes in the medium are also not phase modulated. In the case of quasi-resonance, both normal modes in the medium become phase modulated even in the absence of phase modulation of these modes on the input surface of the medium. In this case, the phase modulation value of the parallel mode in the case of pulses of the considered duration (about 15 ns) turns out to be negligibly small.

If the input probe light is a pulse, then in the medium this pulse splits into pulses, each of which contains the energy of one of the normal modes. The distance travelled by a pulse in a medium prior to its splitting into mode pulses is shorter in the case of quasi-resonance than in the case of strict resonance. In the case of strict resonance, the pulse of the total probe field in the medium phase modulated up to its splitting into mode pulses without phase modulation, even if this pulse did not have phase modulation on the input surface of the sample. In the case of quasi-resonance and in the absence of phase modulation of the input probe pulse, pulses in which the total probe field energy is contained are phase modulated at all stages of their propagation.

It is shown that the transparency of the medium associated with the EIT phenomenon decreases with the transition from the case of strict resonance to the case of quasi-resonance. Moreover, for the perpendicular normal mode, this effect is more significant than for the parallel one.

References

1. Demtröder W. *Laser Spectroscopy: Basic Concepts and Instrumentation* (Berlin, New York: Springer, 2002; Dolgoprudnyi: ID 'Intellekt', 2014).
2. Vitanov N.V., Rangelov A.A., Shore B.W., Bergmann K. *Rev. Mod. Phys.*, **89**, 015006 (2017).
3. Harris S.E. *Phys. Today*, **50**, 36 (1997).
4. Lukin M.D. *Rev. Mod. Phys.*, **75**, 457 (2003).
5. Fleischhauer M., Imamoğlu A., Marangos J.P. *Rev. Mod. Phys.*, **77**, 633 (2005).
6. Duan L.-M., Lukin M.D., Cirac J.I., Zoller P. *Nature (London)*, **414**, 413 (2001).
7. Sinatra A. *Phys. Rev. Lett.*, **97**, 253601 (2006).
8. Martinalli M., Valente P., Failache H., Felinto D., Cruz L.S., Nussenzveig P., Lezama A. *Phys. Rev. A*, **69**, 043809 (2004).
9. Godone A., Micalizio S., Levi F. *Phys. Rev. A*, **66**, 063807 (2002).
10. Lukin M.D., Imamoğlu A. *Nature (London)*, **413**, 273 (2001).
11. Kocharovskaya O., Mandel P. *Phys. Rev. A*, **42**, 523 (1990).
12. Jen H.H., Daw-Wei Wang. *Phys. Rev. A*, **87**, 061802(R) (2013).
13. Basler C., Grzesiak J., Helm H. *Phys. Rev. A*, **92**, 013809 (2015).
14. Ronggang Liu, Tong Liu, Yingying Wang, Yujie Li, Bingzheng Gai. *Phys. Rev. A*, **96**, 053823 (2017).
15. Fam Le Kien, Rauschenbeutel A. *Phys. Rev. A*, **91**, 053847 (2015).
16. Wielandy S., Gaeta A.L. *Phys Rev. Lett.*, **81**, 3359 (1998).
17. Bo Wang, Shujing Li, Jie Ma, Hai Wang, Peng K.C., Min Xiao. *Phys. Rev. A*, **73**, 051801(R) (2006).
18. Agarwal G.S., Dasgupta S. *Phys. Rev. A*, **67**, 023814 (2003).
19. Sautenkov V.A., Rostovtsev Y.V., Chen H., Hsu P., Agarwal G.S., Scully M.O. *Phys. Rev. Lett.*, **94**, 233601 (2005).
20. Tai Hyun Yoon, Chang Yong Park, Sung Jong Park. *Phys. Rev. A*, **70**, 061803(R) (2004).
21. Kis Z., Demeter G., Janszky J. *J. Opt. Soc. Am. B*, **30**, 829 (2013).
22. Parshkov O.M. *Quantum Electron.*, **48** (11), 1027 (2018) [*Kvantovaya Elektron.*, **48** (11), 1027 (2018)].
23. Maneesh Jain, Kasapi A., Yin G.Y. *Phys. Rev. Lett.*, **75**, 4385 (1995).
24. Kasapi A., Maneesh Jain, Yin G.Y., Harris S.E. *Phys. Rev. Lett.*, **74**, 2447 (1995).
25. Saleh B., Teich M. *Fundamentals of Photonics* (New York: Wiley, 1991; Dolgoprudnyi: ID 'Intellekt', 2012).
26. Born M., Wolf E. *Principles of Optics* (Oxford: Pergamon, 1984; Moscow: Nauka, 1970).
27. Parshkov O.M. *Quantum Electron.*, **47** (10), 892 (2017) [*Kvantovaya Elektron.*, **47** (10), 892 (2017)].